

Mémoire de Maîtrise en médecine No

Immune infiltrate in sarcomas

Student

Maxime Ringwald

Tutor

Prof. I. Stamenkovic

Division of Experimental Pathology, CHUV

Expert

Dr D. Golshayan

Center for Immunity and Infection, CHUV

Supervisor

Dr G. Fregni

Division of Experimental Pathology, CHUV

Lausanne, 2015

“Success consists of going from failure to failure
without loss of enthusiasm.”

Winston Churchill

Table of Contents

Acknowledgements	1
Abstract	2
Introduction.....	3
Materials and methods	6
Tumor samples and enzymatic dissociation.....	6
Antibody staining and data acquisition.....	6
Gating strategies	8
Results	13
Overall results.....	13
Myeloid cell characterization	16
T cell characterization	17
Synovial sarcoma	19
Discussion and future perspectives.....	22
References.....	25

Acknowledgements

I am in debt to Professor I. Stamenkovic, who assisted me with the idea of the project and who kindly allowed me perform the work in his laboratory.

I would like to thank Dr D. Golshayan for her assessment of my work.

I am grateful to G. Fregni for supervising my work.

A special thought to my parents, for their unconditional love and support. Last but not least, to my brother, a perpetual source of inspiration.

Abstract

Sarcomas are malignant tumors emerging from mesenchymal tissues including bone, cartilage, adipose tissue and muscle. Sarcomas are rare, accounting for only 2 to 3 percent of all adult cancers. Underlying pathogenic mechanisms are slowly beginning to be understood and in about a third of sarcomas include unique chromosomal translocations that generate fusion genes, which encode fusion proteins most of which function as aberrant transcription factors. However, two thirds of sarcoma harbor complex genetic alterations that preclude clear assessment of their pathogenesis.

Numerous studies suggest that the immune system has an important role in the control of tumor progression. It is documented that patients with tumors having a strong cytotoxic T cell infiltrate have a better overall survival rate than those with tumors that do not. It is also well known that cancer can evade the host immune defenses. Thus it seems important to characterize tumor immune infiltrates and determine their precise role with regard to tumor growth. Unlike other types of cancer, immune infiltrates in sarcomas have been little studied.

The aim of this study is to characterize the phenotype of immune cell populations infiltrating different types of sarcomas. Samples of seven types of sarcomas have been analyzed. Following tumor dissociation, immune infiltrates were analyzed by flow cytometry. Our preliminary results show myeloid cells to be the dominant population, followed by small amounts of T cells. The myeloid population is heterogeneous and is composed of different cell subsets, including macrophages (HLADR+CD11b+) and cells displaying HLADR- plus a combination of CD11b+ CD15+ and CD33+ phenotypes. These cells could correspond to myeloid-derived suppressor cells (MDSCs), which are strongly immunosuppressive and promote tumor growth and metastasis. Different T cell subpopulations have also been found. The dominant subset consists of CD4+ T cells, typically associated with helper functions. Samples with high levels of CD4+ T cells and CD25+Foxp3+ T cell (that correspond to regulatory cells) had low counts of CD4-/CD8+ T cells that are associated with cytotoxic functions.

Immune cell infiltrates in sarcomas are poorly described in the literature. A better phenotypic and functional characterization of these cells could probably help in the development of new therapeutic strategies.

Keywords: cancer, sarcomas, immune infiltrate, fluorescence-activated cell sorting, myeloid-derived suppressor cells.

Introduction

Cancer is a genetic disease that affects people of any age, gender and race. According to the World Health Organization, cancer figures among the leading causes of death worldwide, accounting for 8.2 million deaths in 2012. Cancers are traditionally classified into multiple categories depending on the identity of the affected tissue (carcinomas, sarcomas, leukemias) and their histopathological characteristics (local invasiveness, mitosis, pleomorphic cell nuclei). However, they are now increasingly categorized according to the genetic mutations they bear and associated epigenetic modifications of the genome. Thus, our view of cancer is rapidly changing from a largely descriptive toward a much more functional classification based on rational parameters that underlie the mechanisms according to which they develop and progress. Cancer generally arises from a single cell. One or more mutations are needed in specific genes (proto-oncogenes, tumor suppressor genes, DNA repair genes) to transform a normal cell into a tumorigenic one. Although some genetic mutations are inherited, most cancers arise as a result of the accumulation of new mutations caused by environmental factors including, among others, UV light, radiation, infection, diet and chemicals (Wogan et al., 2004). Tumorigenesis is the process which may occur following transformation of a cell, depending on how the cell responds to transforming agents. Transformation that leads to tumorigenesis provides the cell with multiple new properties such as evading apoptosis, self-sufficiency in growth signals, insensitivity to anti-growth signals, tissue invasion and metastasis, limitless replicative potential and sustained angiogenesis (Hanahan & Weinberg, 2000).

Sarcomas are malignant tumors emerging from mesenchymal tissues, including bone, cartilage, adipose tissue and muscle. Sarcomas are quite rare, accounting for only 2-3% of all adult cancers but up to 15% of pediatric ones. Although new multidisciplinary therapeutic approaches are increasingly applied, the overall survival rate of five years remains strongly compromised if surgery is not curative. Gradually, underlying pathological mechanisms are beginning to be understood, chief among which are unique chromosomal translocations that give rise to fusion proteins, most of which appear to function as aberrant transcription factors or transcriptional regulators as illustrated in Ewing and synovial sarcoma (Riggi et al., 2007a; Riggi et al., 2007b; Suva et al., 2007). But for the vast majority of sarcomas (leiomyosarcoma, high-grade spindle cell sarcoma, myxofibrosarcoma, pleomorphic sarcoma, dedifferentiated liposarcoma and undifferentiated myxofibrosarcoma) underlying pathogenic mechanisms still remain unclear and classification remains primarily based on morphology. According to the French *Fédération Nationale des Centres de Lutte Contre le Cancer* (FNCLCC), the grade of a sarcoma is based on a score - including tumor differentiation, mitotic rate and amount of tumor necrosis. The grade is a sign of how likely the cancer will spread. For example low-grade sarcomas contain well-differentiated cells and tend to disseminate less. Higher-grade sarcomas tend to grow and spread faster than lower-grade counterparts.

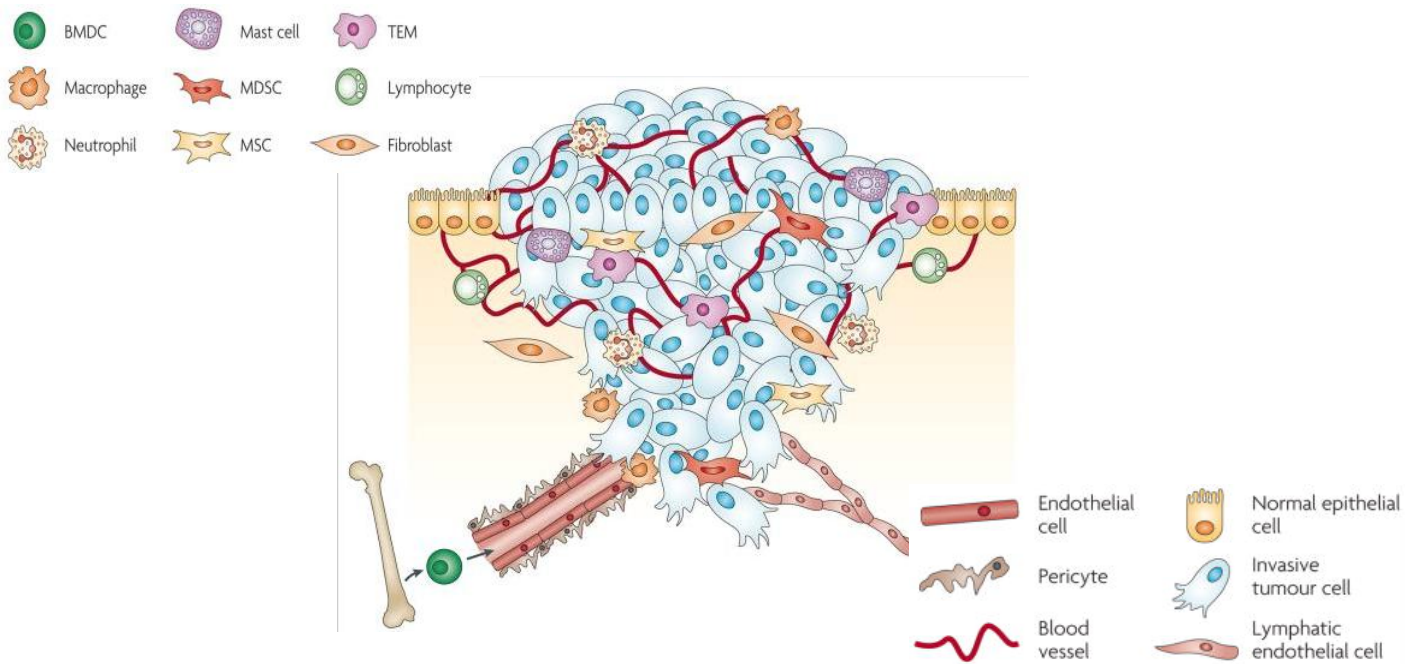


Figure 1. The primary tumor microenvironment (Joyce and Pollard, 2009)

The microenvironment surrounding tumor cells is composed of diverse types of cells including hematopoietic cells such as macrophages, lymphocytes, myeloid-derived stem cells and a variety of stromal cells ranging from differentiated myofibroblasts to mesenchymal stem cells.

Cancer immune surveillance, elimination and escape are old concepts that are beginning to be better understood in light of in-depth molecular and cellular analyses. Cancer is intimately linked to inflammation (Coussens & Werb, 2002), where innate immunity can play the role of a double-edged sword. Numerous studies suggest that adaptive immunity plays an important role as well in the control of tumor progression (de Visser et al., 2006). It is well known that patients with tumors that have abundant cytotoxic infiltrates have a better overall survival rate than do those with tumors that do not (Sorbye et al., 2011; Sorbye et al., 2012; Galon et al., 2006; Galon et al., 2013). Furthermore, new functional sub-populations of immune cells continue to be described (Prendergast & Jaffee, 2013) and contribute to a better understanding of the notion of immune surveillance of tumor behavior (Hanahan & Weinberg, 2011).

Several types of immune cells are important in immune surveillance (Figure 1). Lymphocytes are divided in two major functional groups: B cells and T cells. B cells are the principal effectors in humoral immunity, being responsible for antibody production. T cells can be grouped into several subpopulations: according to phenotypic marker expression, i.e. CD4+, CD8+ and according to their more relevant functional properties. Thus, CD8+ cells have a predominantly cytotoxic role, killing cells by cell-to-cell interactions. CD4+ cells or T helpers are divided into several categories, including Th1, Th2 and Th17. Their role is to interact with other cells of the immune system to promote primarily cell-mediated (Th1) or humoral (Th2) immune responses. T regulatory cells (T regs), discovered during the '90s, are a subset of T helper cells (CD4+), which express CD25+ and transcription factor FoxP3. Their principal role is to inhibit proliferation and function of activated cytotoxic T cells (CD8+) and activated CD4+ T cells at least in part through a cell-to-cell contact dependent mechanism. The ratio CD4/CD8 is important for patient survival. It has been shown that cancer patients with a higher rate of CD8+ cells have a better overall survival than those who do not. In addition to "classical" immune populations of T cells that express only CD4 or CD8, new subsets of

T cells have been described in literature (Thompson et al., 2006). These new populations have a double negative (CD4-CD8-) or double positive (CD4+CD8+) phenotype. NK cells are a small subset of lymphocytes that act similarly to CD8+ T cells and display cytotoxic activity toward virally infected or tumor cells that express low levels of major histocompatibility complex molecules. Unlike T cells, NK cells do not possess specific receptors for tumor antigen recognition in the context of MHC (Moretta et al., 2014).

Another important family of immune cells frequently found at the tumor site are myeloid cells. Monocytes are blood precursors of macrophages. Macrophages are plastic cells, capable of differentiation into at least two distinct populations - M1 and M2 (Martinez & Gordon, 2014). M1 are generally tumor suppressive, producing effector molecules (reactive oxygen species), including cytokines that promote a pro-inflammatory Th1 response. M2 cells promote a Th2 response, which is anti-inflammatory and favors tissue repair and remodeling. This capability can be used by the tumor to model its microenvironment according to its needs. Macrophages can undergo conditioning by tumor cells to become tumor-associated macrophages (TAMs). TAMs display phenotype characteristic of M2 macrophages (secretion of IL-10 and TGF- β) and are unable to trigger Th1-polarized immune response (production of arginase, Zea et al., 2005) but rather induce T regs. They are present in well-established cancer and contribute to direct the local immune system away from antitumor function. TAM-derived factors promote tumor cell proliferation and survival (Chanmee et al., 2014).

A more recently identified functional population of myeloid cells is composed of myeloid-derived suppressor cells (MDSCs), which have strong immunosuppressive activity and are frequently associated with tumor progression (Gabrilovitch & Nagaraj, 2009). Multiple mechanisms of action have been suggested. These cells can protect against autoimmunity but, on the other hand, can also induce tumor promoting effects through modulating the immune functions of macrophages, NK cells, B cells, T cells. MDSCs originate in the bone marrow as CD11b+ hematopoietic precursor cells. MDSCs gene expression is very variable between tumors. Although many studies have been carried out, it is very difficult to identify a unique phenotype of markers. Moreover, mechanisms leading to accumulation of MDSCs in bone marrow and blood of patients are incompletely understood, as well as the direct correlation between MDSCs, chronic inflammation and immunosuppressive state.

Unlike carcinomas, the immune infiltrate in sarcomas has been little studied. In this work, with a selected panel of markers we analyzed the main immune cell populations infiltrating tumor in samples from patients before any treatment.

Materials and methods

Tumor samples and enzymatic dissociation

Eight different tumor samples were included in this study: a leiomyosarcoma (HGS8), a high-grade spindle cell sarcoma (HGS17), a myxofibrosarcoma (HGS18), a pleomorphic sarcoma (HGS19), a dedifferentiated liposarcoma (HGS21), an undifferentiated myxofibrosarcoma (HGS23), a Wilms tumor, even though it is not a sarcoma, and a synovial sarcoma. Approval was obtained from the Ethics Committee of the Canton de Vaud, protocol number 260/15. To obtain a bulk of single cells, fresh samples were put in Petri dishes containing IMDM medium (Gibco) supplemented with 1% of penicillin/streptomycin (PS) antibiotics (Gibco) and mechanically dissociated using a scalpel. Samples were incubated at 37°C for two hours with collagenase type II and IV (0.5 mg/ml, Sigma) and DNase I (100 ng/ml, Roche). To obtain a single cell suspension, dissociated samples were passed through a 70 µm cell strainer. Single-cell bulk samples (tumorigenic cells, immune infiltrate and dead cells) were then frozen and stored in liquid nitrogen. Each sample contained an average of 10^7 cells that were used for FACS staining.

Antibody staining and data acquisition

Stainings have been performed on frozen samples after thawing. Samples underwent multiple washes in IMDM + 1% PS medium followed by resuspension in MACS buffer (PBS 1x-0.5% BSA-EDTA 2mM). To block all unspecific Fc-gamma receptors thus reducing unspecific fluorescence, cells were incubated 20 minutes at 4°C with FcR blocking reagent (human, Myltenyi). Then, they were washed and stained for 30 minutes (4°C) with specific antibodies in a total volume of 30 µl on a 96 V-well-plate. 7AAD and DAPI were used as markers of cell viability.

Molecules	Fluorochrome	Dilution	Purchase from
CD33	eFluor450	1:20	eBioscience
CD11b	APC-eFLuor780	1:20	eBioscience
CD8	Pacific Orange	1:25	exBio
CD16	PerCP-Cy5.5	1:20	BD Pharmingen
CD3	PC7	1:20	Beckman Coulter
CD19	FITC	1:40	eBioscience
CD15	PE	1:20	Beckman Coulter
CD56	ECD	1:40	Beckman Coulter
CD45	Alexa700	1:20	BD Pharmingen
HLADR	APC	1:20	BD Pharmingen
CD4	PE	1:40	BD Pharmingen
FoxP3	FITC	1:1	eBioscience
CD25	APC	1:100	eBioscience
7AAD	ECD	NA	eBioscience
DAPI	NA	1:10000	NA

Table 1. List of antibodies and working dilutions

Four different antibody mixes were used to stain the samples (Joyce & Pollard, 2009). Table 1 shows the list of antibodies, corresponding dilutions previously established in the laboratory and associated fluorochromes. The different antibody combinations are reported in figure 2. Around 10^6 cells per condition were incubated. Mix 1 (CD19, CD14, CD56, CD16, CD3, HLADR, and CD45) was used to characterize the proportions of T cells, NK cells, B cells and macrophages. Mix 2 (CD15, CD3,

HLADR, CD45, CD11b and CD33) was used to characterize myeloid cells (Mirza et al., 2006). T cell subpopulations were analyzed using Mix 3 (CD4, CD56, CD3, CD45 and CD8) and Mix 4 (FoxP3, CD4, CD3, CD25 and CD45). For Mix 4, containing antibodies targeting the FoxP3 nuclear protein, cells were permeabilized using the FoxP3 kit following manufacturer instructions (eBioscience, Anti-Human FoxP3, FITC staining set). A condition without FoxP3 antibody was used as control. Cells stained with anti-CD45 and live/dead markers were used as negative controls (Figure 2).

After incubation, cells were washed, resuspended in 100 µl of MACS buffer and transferred in a tube containing 400 µl of MACS buffer. Cells were kept protected from light and stored at 4°C until FACS acquisition. Stained samples were acquired on a *Gallios Flow Cytometer* (Beckman Coulter) and FlowJo V10 software was used for analysis.

Before data acquisition, voltages were set up using unstained cells. A minimum of 4000 living/single cells was acquired for each sample. To set up compensations, single positive stained beads (BD Comp-Bead Anti-Mouse Ig, k, BD Biosciences) were used to correct for fluorochrome spectral overlap. Compensations were calculated using FlowJo software.

	FL1 (525)	FL2 (575)	FL3 (620)	FL4 (695)	FL5 (755)	FL6 (660)	FL7 (725)	FL8 (755)	FL9 (450)	FL10 (550)
	FITC	PE	ECD	PerCP-Cy5.5	PC7	APC	Alexa700	APC-eFluor780	DAPI	Krome Orange
Unstained (1)										
7AAD (2)			7AAD							
DAPI (3)							CD 45		DAPI	
1st Mix: T, NK, B, Myeloid (4)	CD19	CD14	CD56	CD16	CD3	HLADR	CD45			
2nd Lix: Myeloid (5)		CD15	7AAD		CD3	HLADR	CD45	CD11b	CD33	
3rd Mix: T cell characterization (6)		CD4	CD56		CD3		CD45		DAPI	CD8
Live Dead (7)			7AAD				CD45			
4th Mix: T reg char (8)		CD4	7AAD		CD3	CD25	CD45			
4th Mix: T reg char (9)	FoxP3	CD4	7AAD		CD3	CD25	CD45			

Figure 2. Antibody staining plan

The first line on the top depicts the filters and the corresponding wavelengths that were used in the Gallios Flow Cytometer. The second line indicates to which fluorochrome each antibody of the same column is conjugated. Following lines correspond to the nine antibody mixes used in staining reactions. The first column on the left represents the name of each condition. Green cell correspond to FoxP3 antibody, blue and purple cells are viability markers, respectively DAPI and 7AAD.

Gating strategies

HGS18 sample was chosen as a representative sample to show all gating strategies (Figures 3, 4, 5 and 6).

For all antibody combinations a common procedure was used to gate on the appropriate cell size and discard doublets and dead cells. Cells negative for 7AAD and DAPI stainings were considered as “living cells”. Immune cells were distinguished from tumor cells by their positive CD45 expression. These first four gating steps, “size”, “single cells”, “living cells” and “CD45+”, are critical to limit the non-specific fluorescence in later analysis, especially while targeting CD11b+ cell populations (Kuonen et al., 2010) (Figures 3, 4, 5 and 6).

Specific gating strategies based on cell surface phenotype were then used for the analysis of the different immune cell proportions for each antibody mix. In figure 3, cells expressing CD3 marker among CD45+ cells were considered as T cells and included on “Ly T” gate. Figure 3 also depicts the gating strategy for B cells (red arrows), NK cells (green arrows) and CD14+ population (blue arrows). In the red pathway, the first gate P1, built over CD3- population, targets subpopulations expressing CD19+, a B cell marker. On P1 population, P2 gate discards cells expressing whether CD16 or CD14, which are markers of monocytes, NK cells and macrophages. “Ly B” selects cells with a CD19+CD56- phenotype. The green pathway represents the gating strategy for NK cells. P3 is the second gate built over CD3- population. It eliminates antigen-presenting cells selecting only cells negative for HLADR expression. NK cells were then considered as CD56+CD16+/- cells. In the blue pathway on the right, CD14+ cells were selected after discarding CD16-/CD14-CD56+ cells by gate P4, and looking at the positive expression of HLADR markers on CD14+ cells. Figure 4 shows the characterization of CD11b+HLADR+ macrophages and the characterization of different subsets of myeloid populations: HLADR-CD11b+/-, CD15+/-, and CD33+/- . The second mix of antibodies was used. Once the CD3- population was obtained, the first gate was built by targeting CD11b+HLADR+ over CD3- population (blue pathway). On the right side of the figure (green pathway), first, HLADR+ and then CD11b-CD33- cells were discarded (“HLADR-“, “CD11bCD33” gates). The expression of CD15 and CD33 markers was then evaluated on CD11b+CD33+/- cells. CD4+, CD8+, CD4-CD8- and CD4+CD8+ T cell subsets were analyzed on CD3+ population using the gating strategy depicted in Figure 5. Proportions of Foxp3+CD25+ T reg cells were analyzed using the gating strategy of Figure 6 among CD3+CD4+ cells.

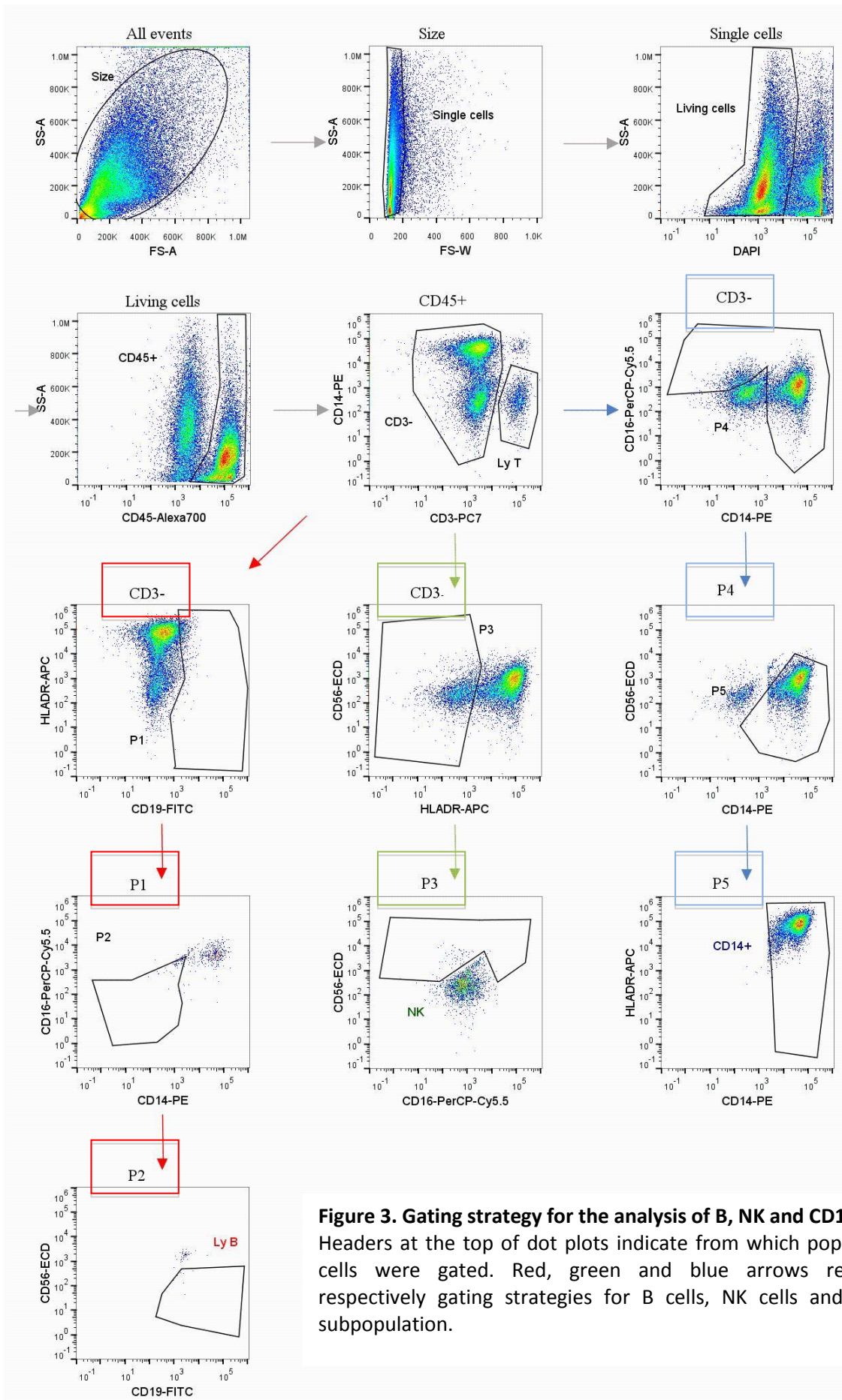


Figure 3. Gating strategy for the analysis of B, NK and CD14+ cells
 Headers at the top of dot plots indicate from which populations cells were gated. Red, green and blue arrows represent respectively gating strategies for B cells, NK cells and CD14+ subpopulation.

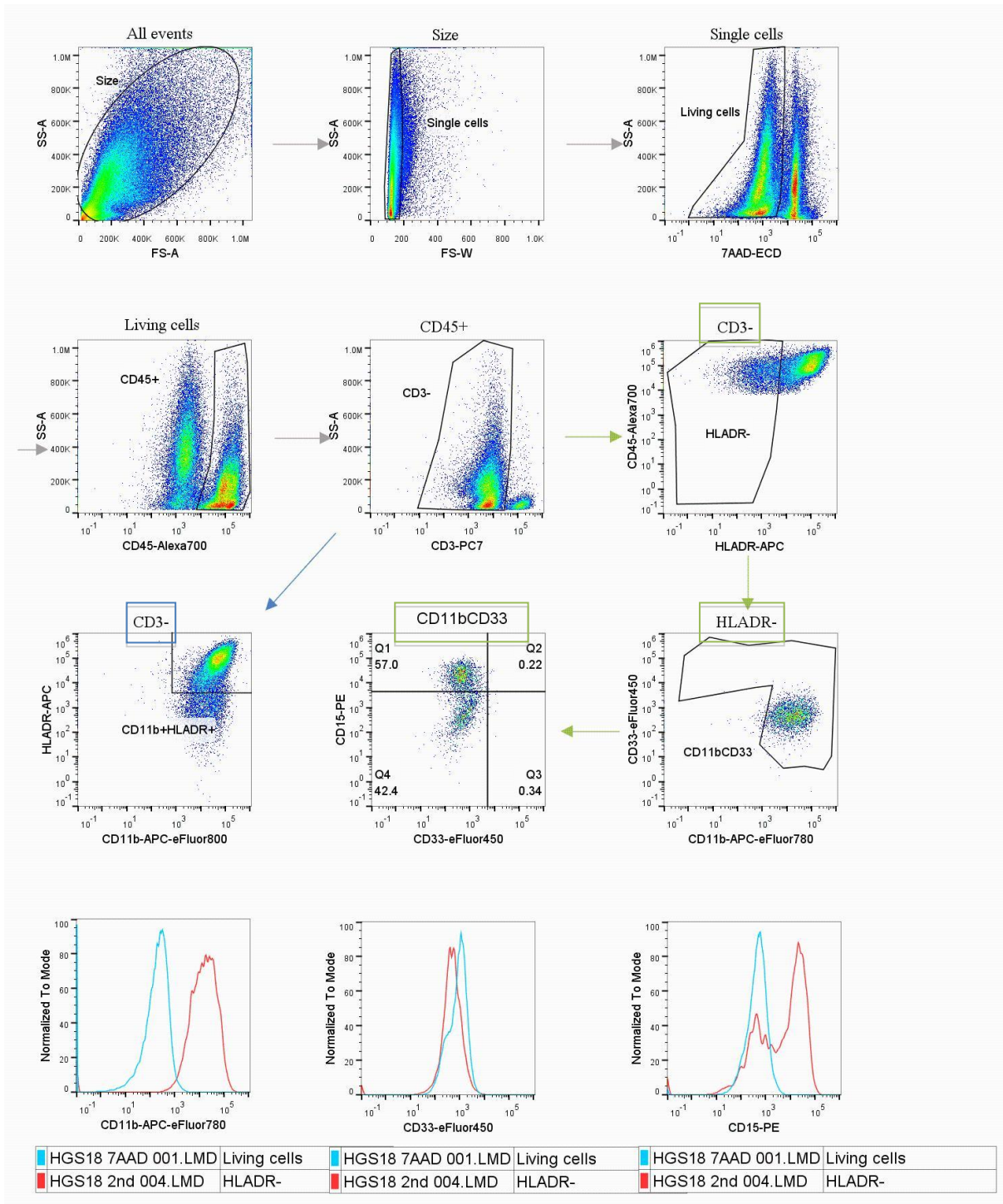


Figure 4. Myeloid cell characterization: gating strategy

Headers at the top of dot plots indicate from which populations cells were gated. Blue and green arrows represent respectively gating strategies of macrophages and myeloid subpopulations. Histograms at the bottom show the expression of CD11b, CD33 and CD15 on HLADR- cells (red lines). Cells stained only with 7AAD were used as negative controls (blue lines).

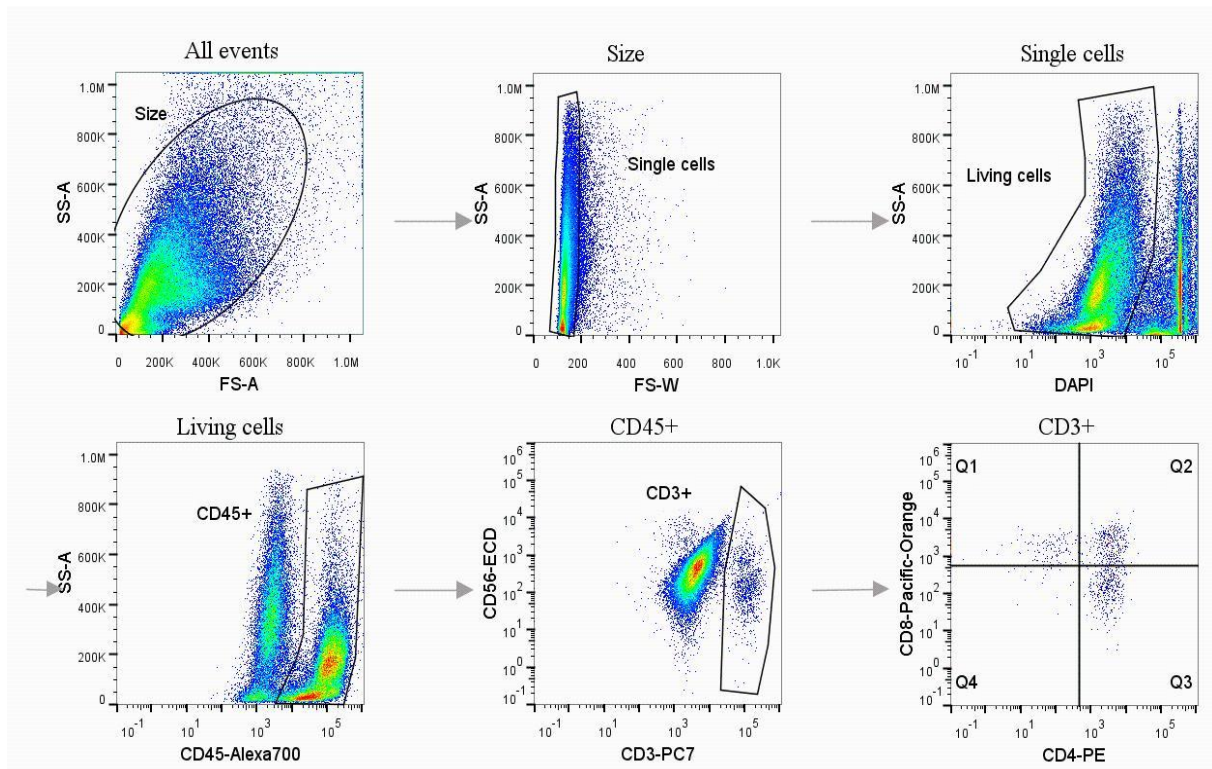


Figure 5. Gating strategy for the characterization of T cell subpopulation

Headers at the top of dot plots indicate from which population cells were gated. CD4+ and CD8+ cell proportions were analysed among CD3+ populations.

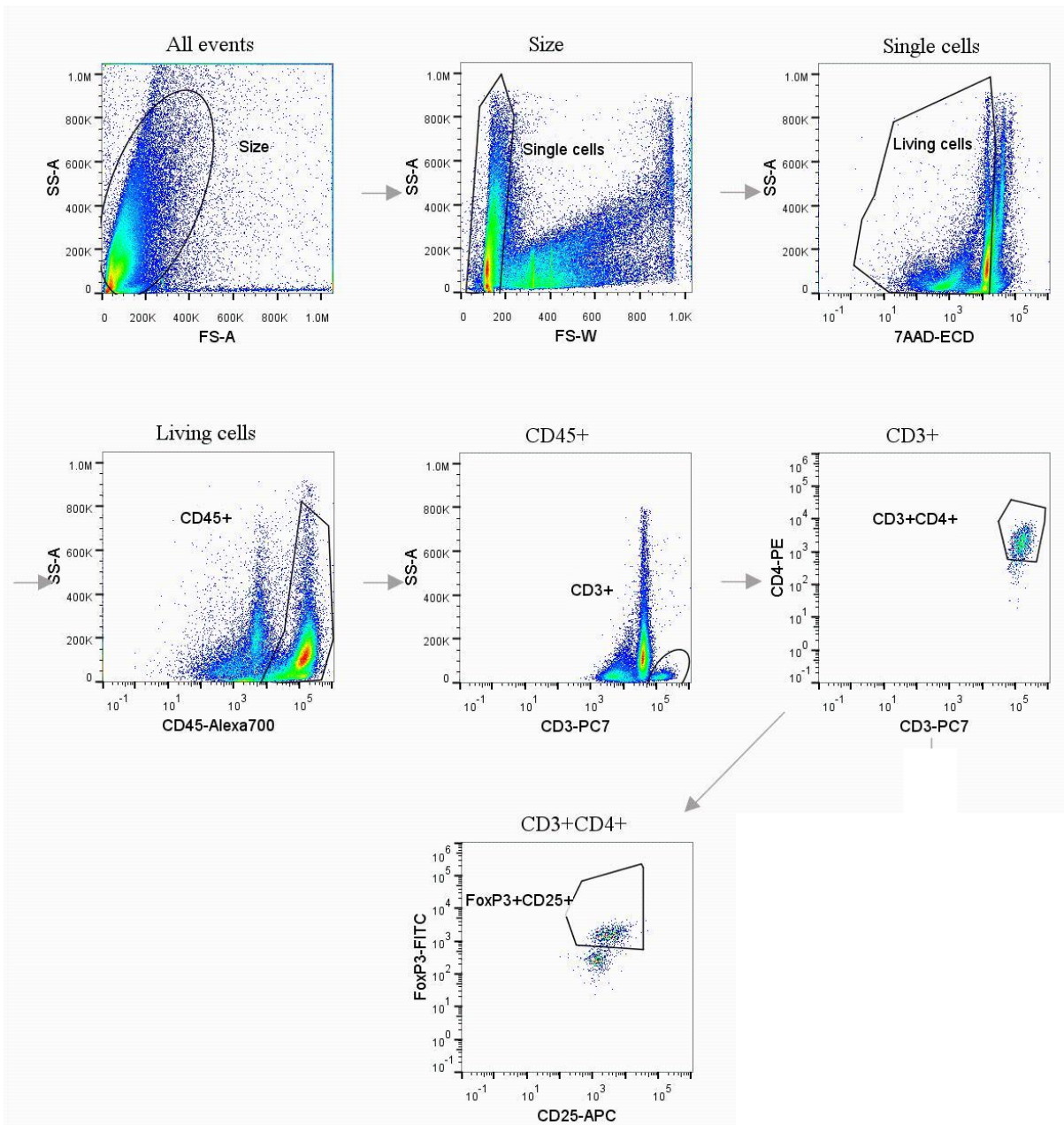


Figure 6. Gating strategy for the characterization of T reg cell proportions
 FoxP3+CD25+ cells among the CD3+CD4+ population were considered as T regs.

Results

Overall results

Eight primary tumor samples were analyzed: high-grade spindle cell sarcoma (HGS17), myxofibrosarcoma (HGS18), pleomorphic sarcoma (HGS19), dedifferentiated liposarcoma (HGS21), undifferentiated/myxofibrosarcoma (HGS23), leiomyosarcoma (HGS8), Wilms tumor and synovial sarcoma.

Wilms tumor is the most common childhood malignancy. Its pathogenesis lies within the mutation of a tumor suppressor gene (WT1). This gene encodes a transcription factor implicated in normal kidney and gonadal development. With current therapies, overall survival is around 80-90% (Davidoff, 2012).

Because of the heterogeneity of the samples, Wilms tumor will be compared to the average of the high-grade spindle cell sarcoma group (HGS), while the synovial sarcoma will be presented separately. Indeed, for this last sample the CD45 staining was not able to discriminate between immune and tumor cells, most likely because of non-specific fluorescence or aberrant expression by tumor cells.

Numbers of living cells were heterogeneous among samples, varying from 33% of single cells (1.7×10^4 cells) in HGS17 sample to 83% (9×10^4 cells) in HGS 21 sample (Figure 7). Compared to the mean value in the high-grade sarcoma group (64%), Wilms tumor displayed a lower amount of living cells representing 40% of the single cell population (4×10^4 cells).

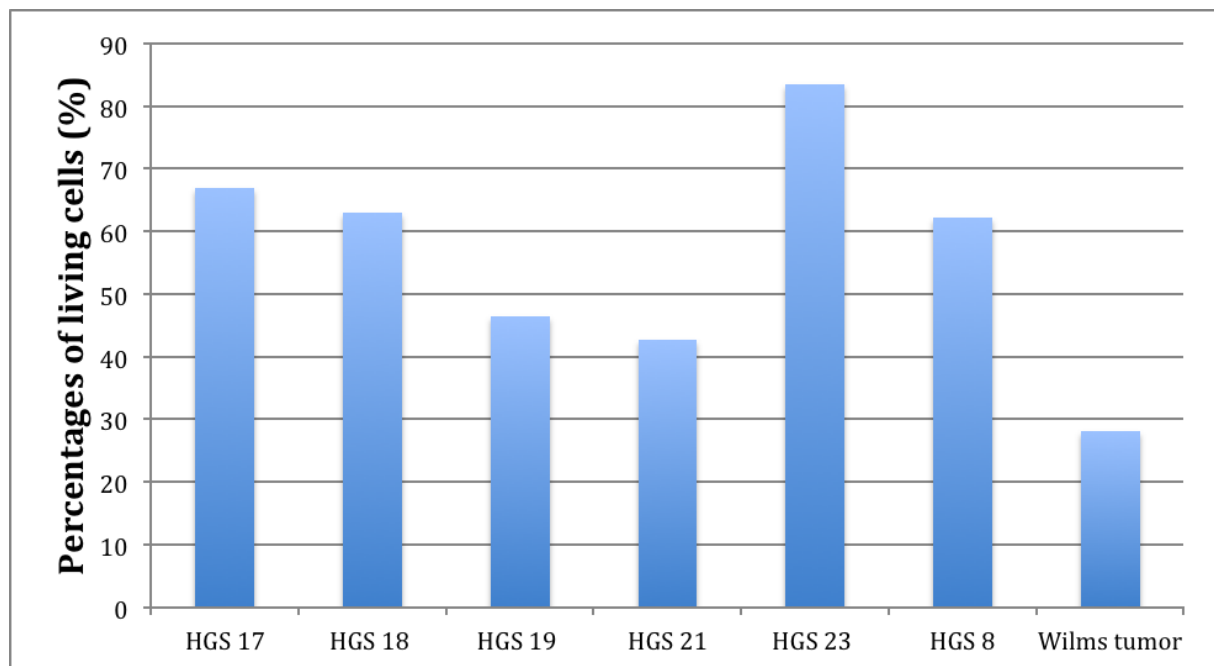


Figure 7. Percentages of living cell population in bulk samples

As discussed previously, CD45, a general marker of immune cells, was used to discriminate immune cells from other cell types, such as endothelial or tumor cells. Figure 8 shows the proportion of immune infiltrates among cell bulk in all samples. Immune cell infiltrates were heterogeneous. With the exception of Wilms tumor sample for which the immune infiltrate represented 30%, immune cell infiltrates were generally abundant and ranged between 43% and 83% of living cells (average of 56% of living cells).

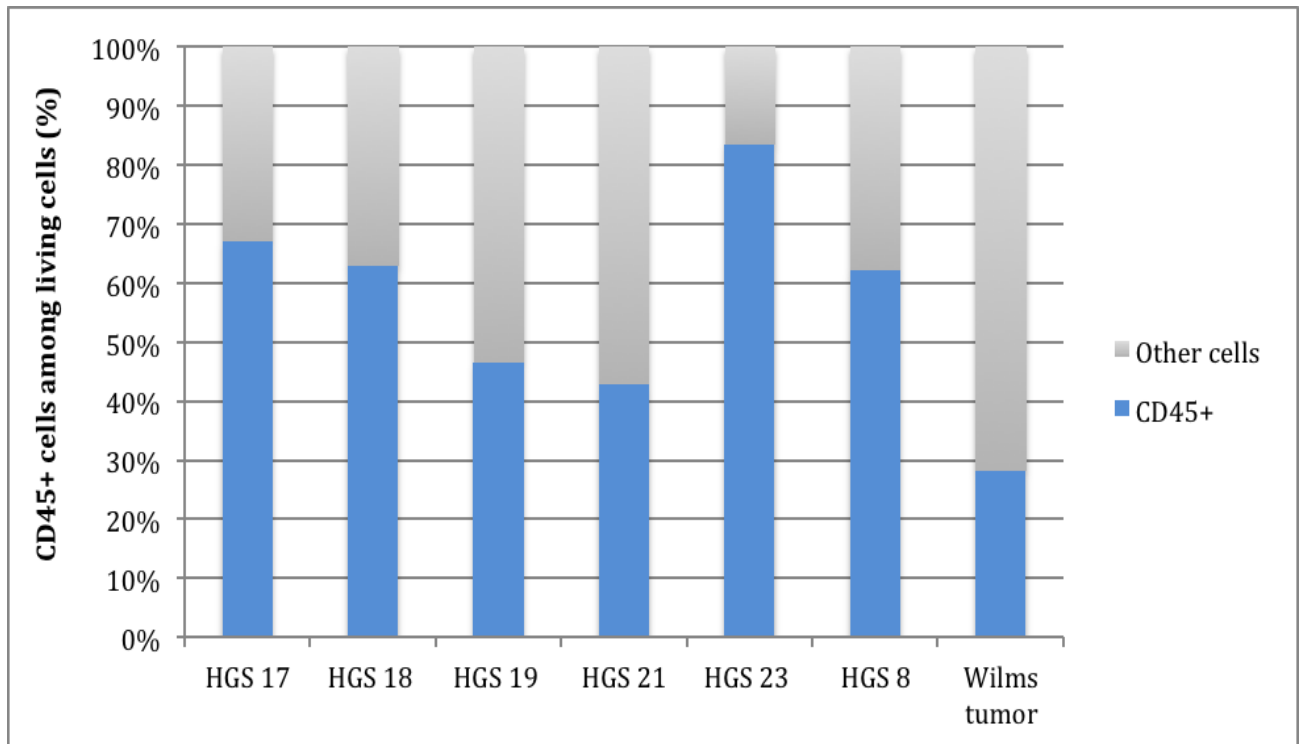


Figure 8. Percentages of total immune cells infiltrating sarcoma

CD3 antigen was used to further characterize T cells among immune infiltrates, whereas B cells, CD14+ cells, other myeloid cells and NK cells were analyzed within the CD3- population. In high-grade sarcoma samples, CD3- population was abundant and ranged between 55.3 and 98.3% of CD45+ immune cells. The proportion of CD3- cells was significantly lower in the Wilms tumor sample (around 10%, Figure 9).

B cell infiltrates were rare. HGS17 and HGS8 tumors showed higher proportions compared to the average of other samples (0.14%), respectively 0.3% and 0.4%. The Wilms tumor displayed a similar B cell percentage as HGS18, HGS19, HGS21 and HGS23 tumors (Figure 10A). NK cells showed a similar distribution, with HGS17 and HGS8 tumors harboring higher proportions than other samples (Figure 10B). Regarding CD14+ cells, proportions were generally low (average of 6.28%), except for HGS18 (38%). Wilms tumor was comparable to other samples with a CD14+ cell component of 0.9% (Figure 10C). Compared to other populations, T cell proportions were higher but nevertheless heterogeneous, with an average of 5.4%. Wilms tumor was characterized by a 10% T cell content (Figure 10D).

Assessment of Wilms tumor results in more detail revealed that adding percentages of CD3+ cells and CD3- cells did not reach 100%. These results could be explained either by experimental errors (e.g. suboptimal staining) or by the fact that our gating procedure was not sufficiently discriminating with respect to live versus dead cells or single cells.

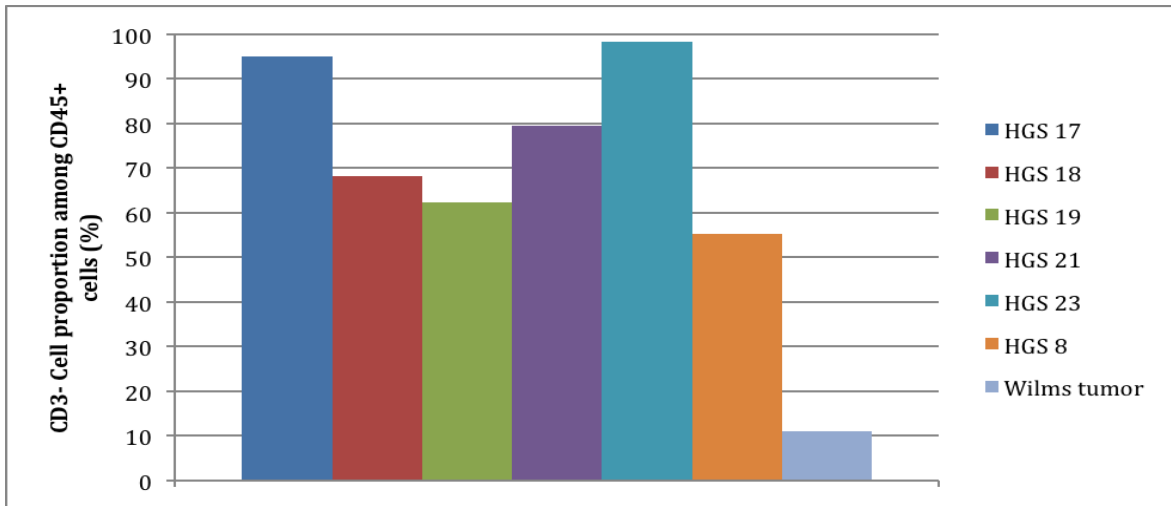


Figure 9. Percentages of CD3- population among CD45+ cells

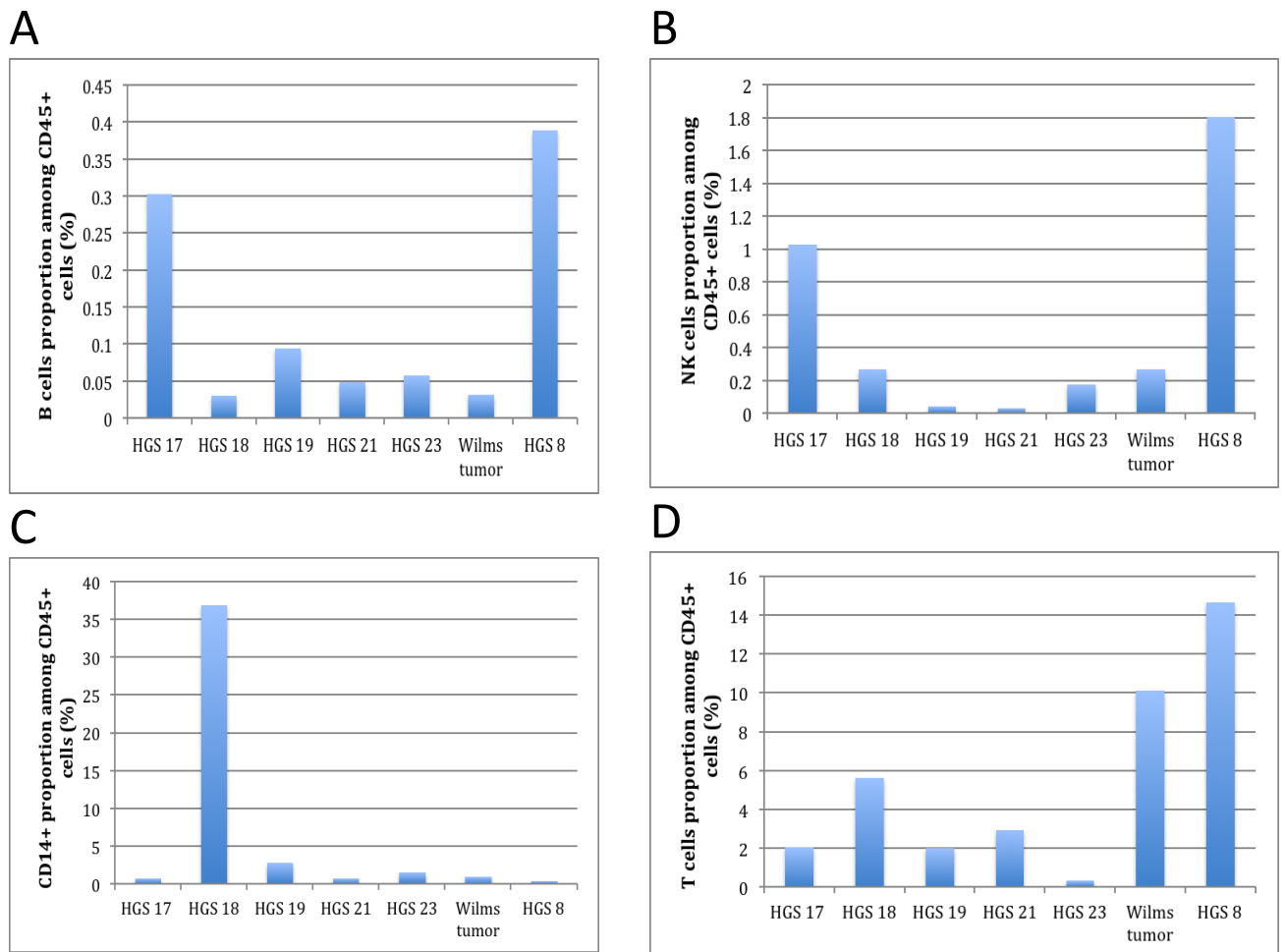


Figure 10. Percentages of B cells (A), NK cells (B), CD14+ cells (C) and T cells (D) among CD45+ cells

Myeloid cell characterization

Myeloid cells were analyzed among the CD3⁻ population using the antibody combination Mix 2 (Figures 2 and 4). Two major phenotypes were characterized: HLADR⁻ cells and CD11b+HLADR⁺ cells, which correspond to a macrophage-like phenotype. HGS18 and HGS19 samples displayed the highest proportion of macrophages, 58.8% and 63.6%, respectively. In Wilms tumor, the percentage of macrophages was 37.1%, which is slightly inferior to the average of sarcomas (45.5%).

Regarding HLADR⁻ cells, results were heterogeneous ranging from 15.6% in HGS18 to 63% in HGS17. The average of all samples was slightly more than 30%. Wilms tumor showed a smaller proportion of HLADR⁻ cells than the average of sarcoma samples (24%)(Figure 11).

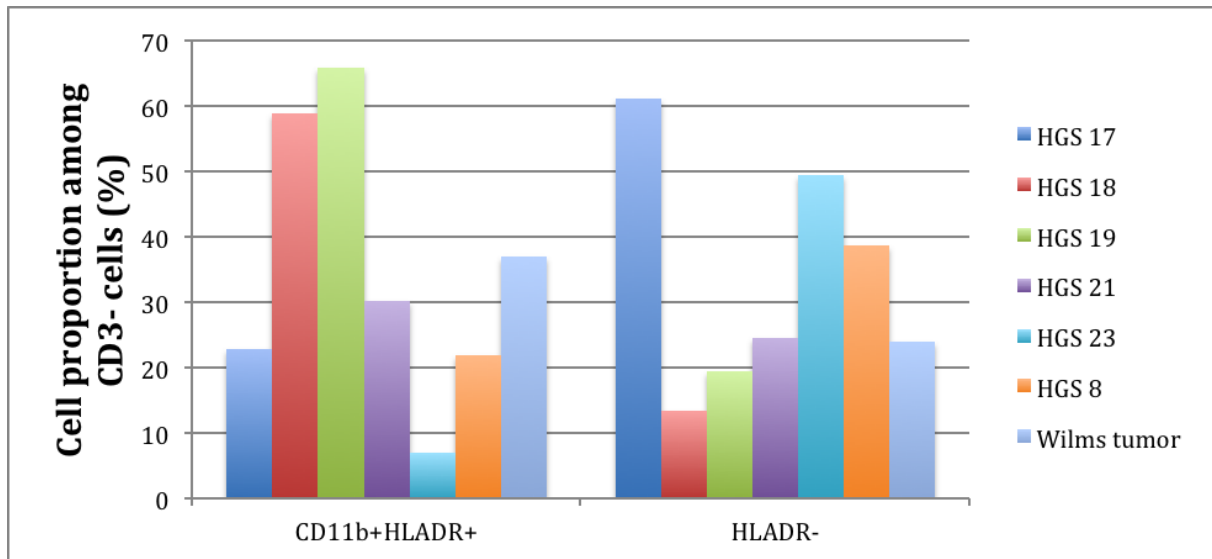


Figure 11. Percentages of HLADR⁻ and HLADR⁺ myeloid cells populations

We analyzed the expression of CD11b, CD15 and CD33 markers among HLADR⁻ cells. These markers have been reported to be associated with MDSCs phenotypes. The vast majority of HLADR⁻ cells expressed CD11b (range 89.3-97.8%, average being 93.3 %)(Figure 12). Compared to sarcomas, Wilms tumor showed a lower proportion of HLADR-CD11b+ cells (64.1%). We then looked at CD33 and CD15 expression among HLADR-CD11b+ populations (Figure 13). Three patterns emerge from these results. The largest population in HGS17, HGS21, HGS23 and HGS8 samples were cells expressing only CD11b (CD33⁻CD15⁻)(purple bars). In these samples a smaller proportion of CD33⁺CD15⁺ cells was also present (blue bars). The second pattern corresponds to HGS 18 and HGS 19 samples for which proportions of CD33⁺CD15⁺ and CD33⁺CD15⁻ were comparable and both close to 50%. Wilms tumor showed a third pattern different from sarcoma samples. The largest populations were characterized by CD33⁺CD15⁻ cells (green bar, 41%) and CD33⁻CD15⁻ cells (39%). CD33⁺CD15⁺ cells represented almost 15% of HLADR-CD11b+ cells and a non-negligible population of double positive CD33⁺CD15⁺ cells (red bar) was also present.

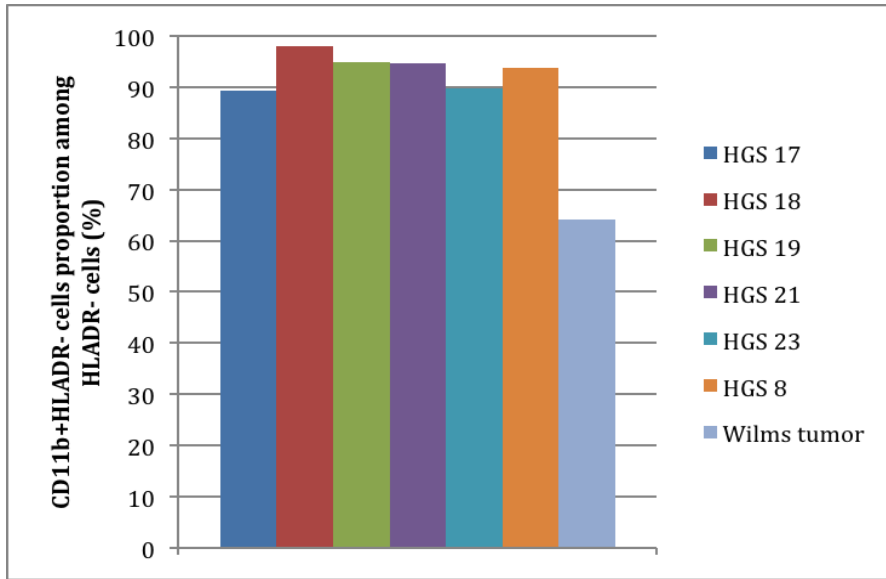


Figure 12. CD11b expression among HLADR- cells

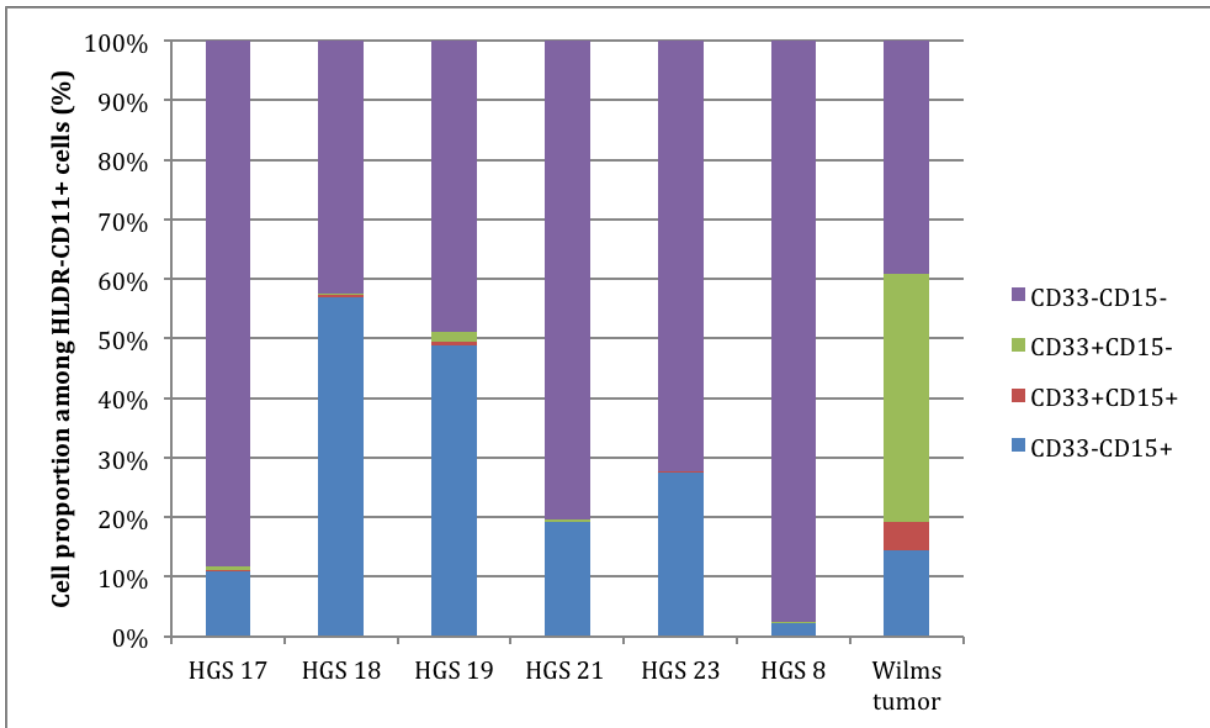


Figure 13. Distribution of cells according to the expression of CD33 and CD15 among HLADR-CD11b+ cells

T cell characterization

Figure 14 represents populations of cells expressing CD4 and CD8 and gives a general overview of T cell characterization. With the exception of HGS17, for which CD4+ proportion was dominant, other samples showed similar proportions of CD4+ and CD8+ T cells. However, proportions of CD4+ added to those of CD8+ correspond to more than 100% (especially for HGS18 and HGS19), suggesting the presence of double positive cells. Double positive populations will be analyzed more in detail through figure 15.

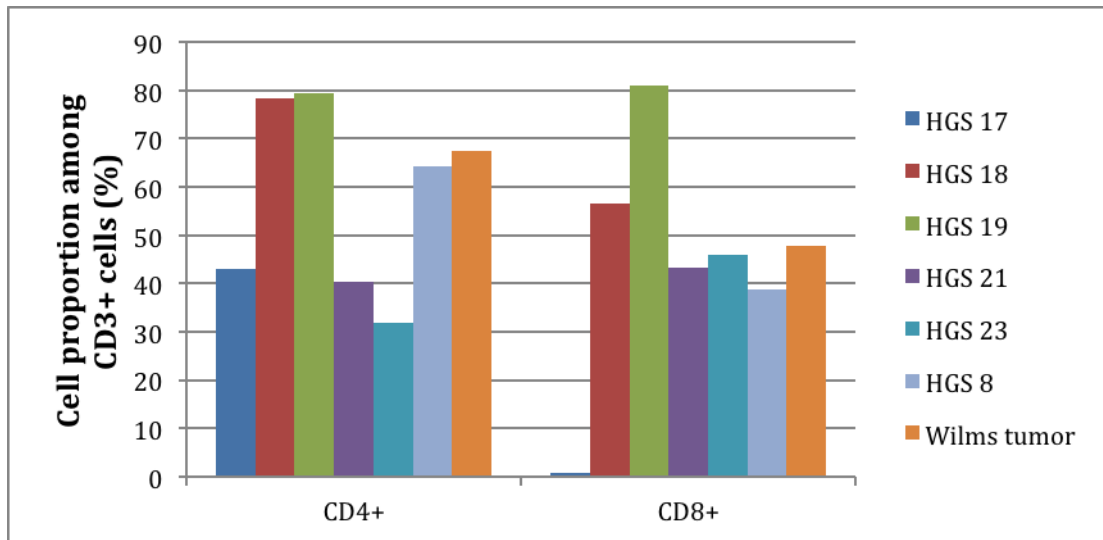


Figure 14. General proportions of CD4+ and CD8+ T cells

It is important to highlight the observation that HGS17 displayed a unique pattern, with the absence of CD8+ and double positive cells. Wilms tumor displayed a similar phenotype compared to the average of CD4+ and CD8+ cell proportions in sarcoma samples, respectively 67% and 48%.

Double negative lymphocytes (red bars) are dominant in HGS 17 and HGS 23, whereas double positive cells (purple bars) are high in HGS 19 and, to a lesser extent, in HGS 18. CD4+ single positive populations (green bars) are the largest in samples HGS18, HGS8 and Wilms tumor; whereas CD8 single positive populations (blue bars) are present in all samples but totally absent in HSG17. There are more samples with a positive CD4:CD8 ratio ($CD4 > CD8$): HGS17, HGS18, HGS8 and Wilms tumor. Remaining samples (HGS19 and HGS 23) have a negative CD4:CD8 ratio ($CD4 < CD8$) or shown a high double positive population.

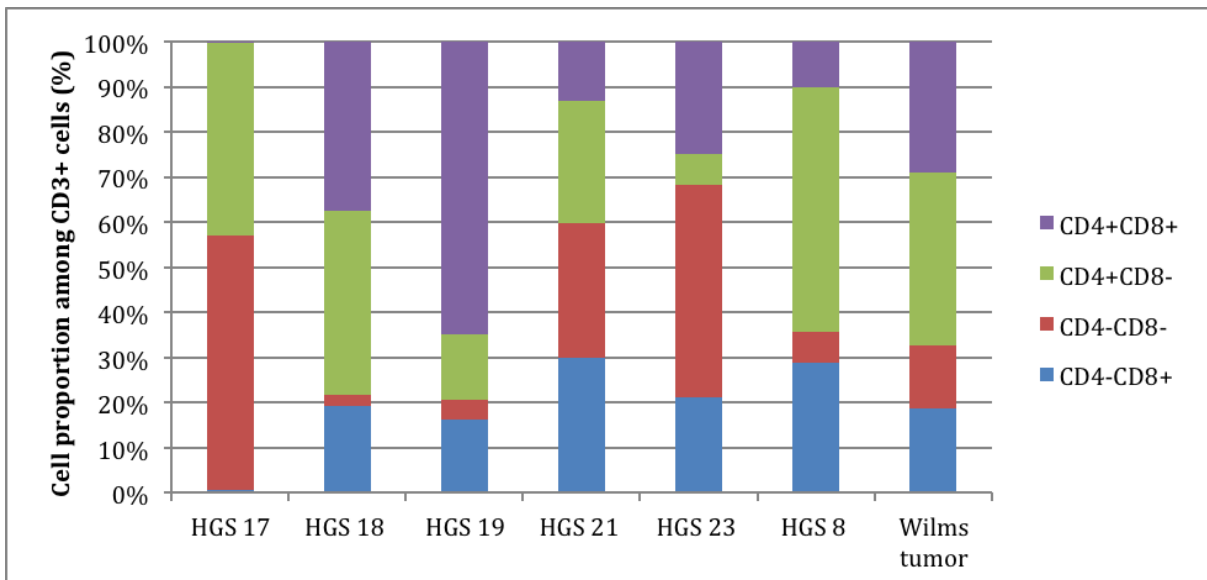


Figure 15. Distribution of lymphocytes regarding the expression of CD4 and CD8 surface marker

Proportions of T reg-like cells ($CD4+CD25+FoxP3+$) were also analyzed among CD3+ cells. Large proportions of T regs are present in HGS17 and in HGS18 samples (Figure 16). Proportions of T regs in HGS19 and HGS23 are lower and close to 5%. In other samples, T reg populations were

smaller. By comparing percentages of CD4+ cells to those of T reg (CD4+CD25+FoxP3+), T regs represented between 5% (HGS8) and 50% (HGS8). The hypothesis that T regs represented a major population of CD4+ can be made.

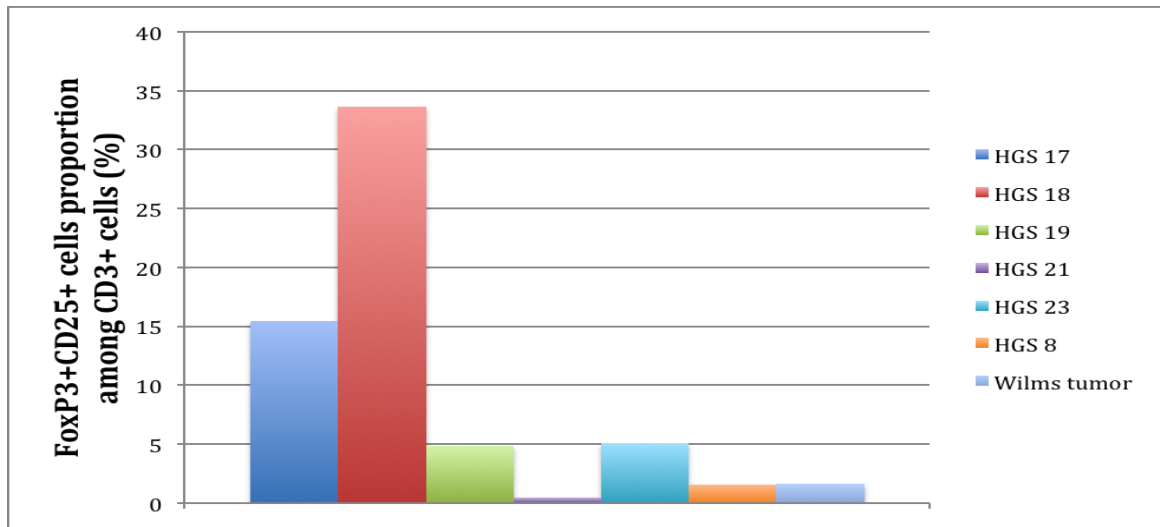


Figure 16. Proportion of T regs among CD3+ population

Synovial sarcoma

Synovial sarcoma showed a different pattern concerning CD45 expression for which the proportion was higher than 90%. It is possible that tumor cells expressed CD45 making our analysis difficult. For this reason, we decided to show the analysis of this sample separately.

By comparing figure 17 with figure 3, populations in figure 17 were not clearly distinguishable and discrimination between negative and positive populations was impossible. These results strongly suggest that the tumor may express CD45. Moreover, it is possible that the tumor also expressed CD56 and possibly HLADR (gates P1 and P3). Nevertheless, we tried to analyze immune cell subpopulations. No CD3+, NK cells, B cells or CD14+ cells were found (Figure 17). We only detected a small population of HLADR+CD11b+ (around 15%) as well as CD11b+CD33+ cells (approximately 33%), which were likely myeloid cells (Figure 18).

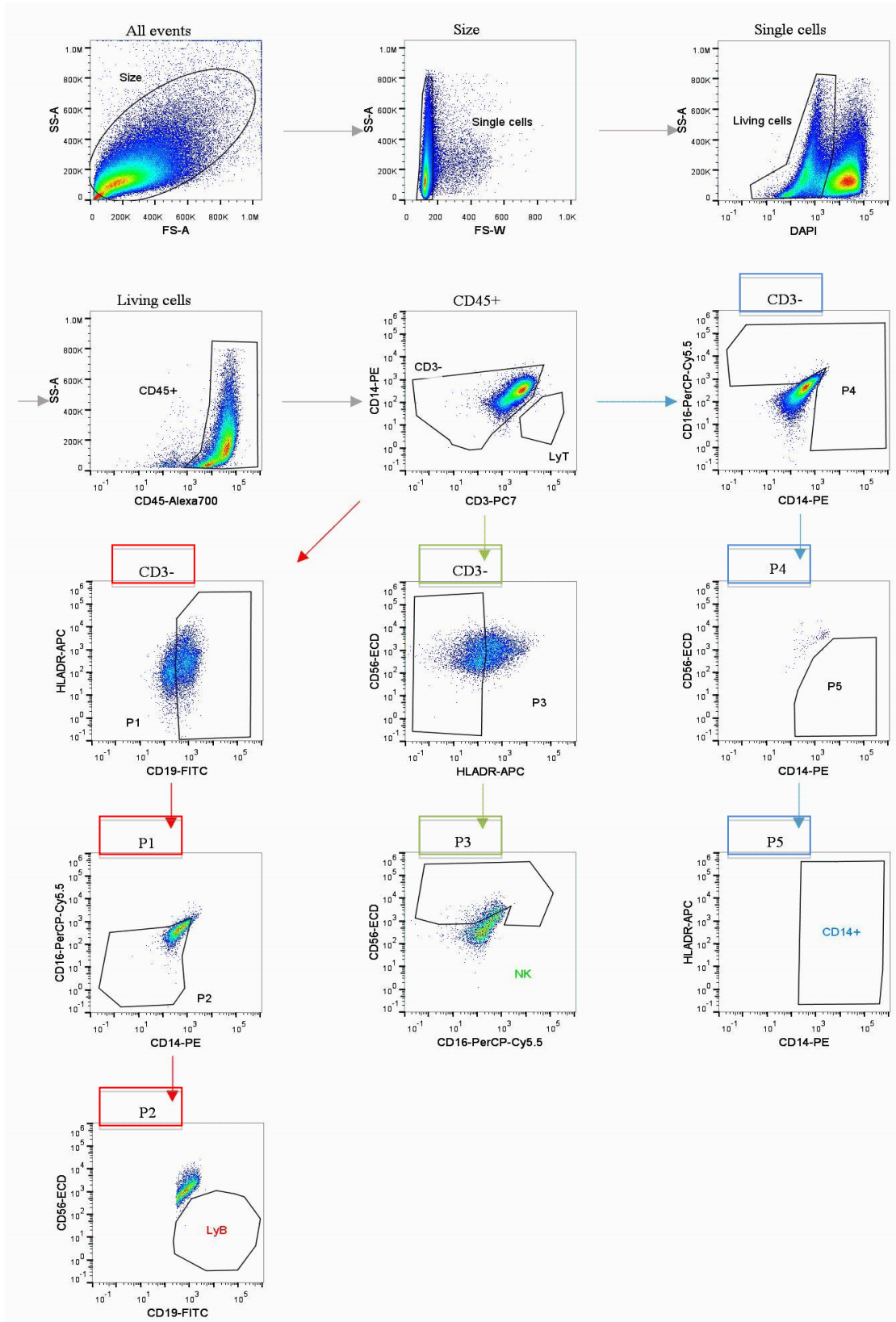


Figure 17. Synovial sarcoma: characterization of B cells, NK cells and CD14+ cells

Headers at the top of dot plots indicate from which populations cells were gated. Red, green and blue arrows represent respectively gating strategies of B cells, NK cells and CD14+ subpopulation.

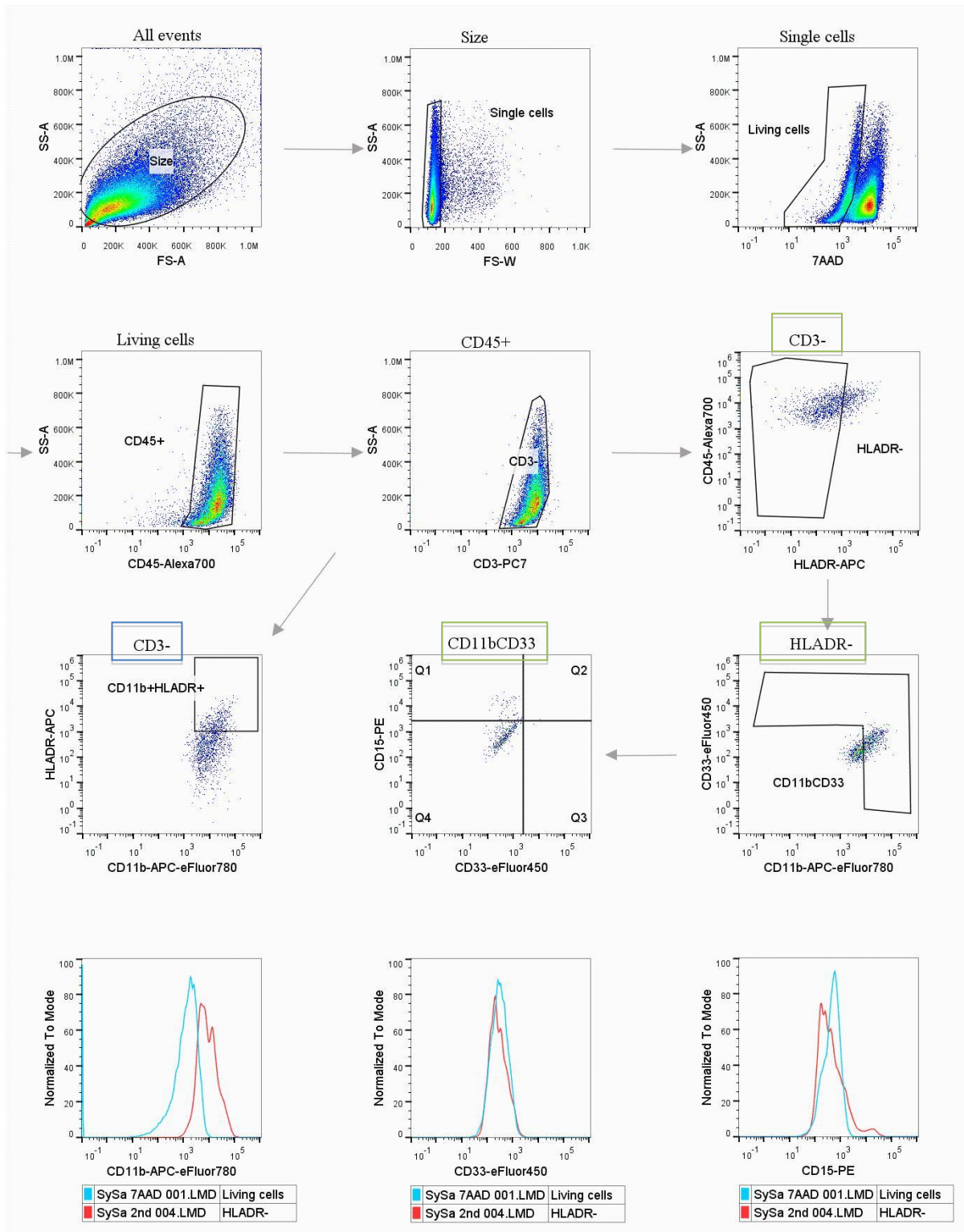


Figure 18. Myeloid cells characterization in synovial sarcoma

Headers at the top of dot plots indicate from which population cells were gated. Blue and green pathways represent respectively gating strategies of macrophages and myeloid subpopulations. Histograms at the bottom show the expression of CD11b, CD33 and CD15 in HLADR⁻ cells (red lines). Cells stained only with 7AAD were used as negative controls (blue lines).

Discussion and future perspectives

Through this study, we characterized immune infiltrates in different types of high-grade sarcomas and in a primary sample of Wilms tumor. Each sarcoma displayed a different pattern in terms of size and composition of immune infiltrate, but one common feature was that dominant populations in each sample were myeloid cells and T regs.

Because of the different nature of the samples, we chose to discuss Wilms tumor separately and compared it to the average pattern of sarcoma samples. Even if some results were comparable, Wilms tumor displayed a unique pattern. Its total immune infiltrate (CD45+ cells) as well as the proportion of CD3- cells was lower compared to the average of sarcomas (Figures 8 and 9, respectively). Moreover, it also displayed a different pattern of CD11b+HLADR- myeloid cells (Figures 12 and 13). T cell infiltrate was higher compared to the average of sarcoma samples (Figure 10D) and mainly characterized by CD4+ cells. However, the proportion of T reg cells was low (Figures 14, 15 and 16).

Myeloid cells are mainly composed of MDSC-like cells and macrophages. MDSCs have been described as immunosuppressive cells (such as interference with T cell function) (Solito et al., 2014) with heterogeneous phenotypes that vary among different types of cancer (Gabrilovitch & Nagaraj, 2009). Certain markers were selected, based on available studies, which seemed recurrent and present in different tumors: renal cell carcinoma (HLADR-CD11b+CD15+) (Zea et al., 2005), head and neck squamous cell carcinoma (HLADR-CD33+)(Almand et al., 2001) and carcinomas in general (CD15+)(Schmielau et al., 2001). As seen in the results, it could be said that there is “a phenotype per sample” and it may reflect and underlie the heterogeneity and complexity of cancer biology (Smith et al., 2013; Young et al., 2001). Throughout this study we did not focus on the association between immune cell infiltrates and clinical stages of patients. It would be interesting to correlate immune infiltrates with clinical stage and immunohistochemistry markers on one hand and genetic patterns on the other, to clinical data as it has been done in some studies (Gentles et al., 2015).

It is important to keep in mind that MDSC is a functional characterization and no functional tests have been performed yet. Moreover, MDSC function has been studied in carcinomas and little is known about MDSCs in sarcomas and even less in the sarcomas used in this study. Different sets of markers are probably needed to characterize MDSCs in more detail in sarcomas. From the general results of this study, there is an inverse correlation between T cell and CD3- cell counts (data not shown). This could possibly be explained by the ability of MDSCs to interfere with T cell functions. However, more experiments need to be conducted to prove or invalidate such hypotheses, but it is conceivable that these cells are MDSCs with an immunosuppressive profile.

Macrophages are the other important subset constituting CD3- populations. Macrophages have been characterized as CD14+ and HLADR+CD11b+ populations (Ruffell et al., 2012). TAMs are often found in large quantities in tumor microenvironments, promoting cancer growth and spread (Kumar et al., 2010). It has recently been shown (in mammary cancers) that macrophages have multiple roles in cancer. By secreting IL-10, macrophages affect the normal function of cytotoxic T cells. Moreover, M2 macrophages, induced by Th2 responses, have been shown to be pro-metastatic. Research using mouse models has shown that suppressing triggers of macrophage differentiation could prevent metastatic states and increase T cytotoxic cell counts. These mechanisms are thought to act not only through secretion of IL-10 but also through mechanisms mediated by myeloid cells, which are not fully understood (Ruffell, personal communication, EPFL lecture 2014). According to the procedures and results of this study, it is not possible to conclude the specific polarization of macrophages towards M1, M2 or TAM. For this purpose, functional studies would be required. In future experiments, it would be interesting to use fresh samples and to

quantify the secretion of IL-10 and determine whether these mechanisms are also found in sarcomas.

Tumor infiltrating lymphocytes are considered to be an indication of the immune reaction of the host and an estimation of the overall expected survival. It is well known that the presence of numerous CD8+ cells is associated with better survival prospects (Weinberg, 2013; Sorbye SW et al., 2011). In samples with large CD4+ cell counts; there are also large counts of FoxP3+CD25+ cells, known as T regs. Under normal conditions, T regs account for 5 to 10% of total CD3- cells and can be augmented in some tumors (Prendergast & Jaffee, 2013). Results found in this study are close to those found in existing literature. T regs are known to be immunosuppressive and tissue repair promoting, thus enhancing tumor proliferation (Danese & Rutella, 2007). Although recent studies have shown that T regs are not automatically associated with poor prognosis and tumor immune evasion, it is recognized that a high T reg count is associated with tumor progression (deLeeuw et al., 2012).

Some other populations have been characterized in past years. Double negative (CD4-CD8-) and double positive (CD4+CD8+) T cells have been described in recent studies (D'Acquisto & Crompton, 2011; Thomson et al., 2006). Although their functions remain very controversial, it seems that these populations could have an immunosuppressive role (Hillhouse & Lesage, 2013; Young et al., 2003).

Results of synovial sarcoma were difficult to analyze because of the diffuse expression of CD45 marker - either the immune infiltrate was dominant or the tumor also expressed this marker. According to the results of this study and the difficulties to better characterize immune cell subpopulations, it seems likely that the tumor is expressing CD45. This condition, although extremely rare, has been reported in literature under some circumstances of undifferentiated tumor or metastasis (Danbara et al., 2009). Other investigations (real time PCR and other FACS analysis) will be performed on this sample. One hypothesis might be that this mechanism of CD45 overexpression is implicated in tumor immune evasion, which may contribute to the poor prognosis of synovial sarcoma (Kerouanton et al., 2014).

Results published early this year underline the importance of translational research and bringing discoveries from bench to bedside. By blocking CSF-1 (which is an activating trigger of macrophages) it has been shown that the tumor bulk was reduced in size and that more T cytotoxic cells were recruited to the tumor site (Ruffell, personal communication, EPFL lecture 2014). This is an example of how targeting specific populations or cytokines could provide potential future therapeutic options.

For this study we used thawed primary samples that had been frozen after tumor dissociation. Analyses on this kind of samples are usually technically difficult because of the heterogeneity of the sample, abundant dead cells and auto fluorescence (Kuonen et al., 2010). In our samples, proportions of living cells among single cells were important (Figure 7), but bulk populations also contained numerous dead cells likely due to, among others, areas of necrosis, tumor dissociation and thawing steps. For these reasons, the first part of the gating procedure, consisting in dead cells removal and doublets discarding, was necessary to eliminate fragments and dead cells allowing us to reduce nonspecific signal in the following steps of phenotypic analysis. Moreover, to further reduce nonspecific staining due to non-specific binding of antibodies to cells, cells were incubated with a FcR receptor blocking reagent. Autofluorescence and unspecific signal could also explain in part the dominant CD45+ pattern we found in the synovial sarcoma sample.

Despite the fact that bulk populations contain numerous dead cells, the immune infiltrate is prominent (> 40%). It is composed mainly of cells with an MDSC-like phenotype, macrophages and subsets of T cells (T regs, double negative and double positive). Other cell types are associated with immune infiltrate and seem to play a role in cancer but little is known about their functions (monocytes, Th17).

To complete the characterization of these populations, it would be necessary to use different sets of antibodies to target cells more precisely. It would be interesting, to use fresh samples to study the function of characterized cells and examine whether macrophages display M1 or M2 properties. MDSC is a functional label. Therefore, it would be also necessary to characterize more in detail putative MDSCs associated with sarcomas, to isolate them and confirm their immunosuppressive function through culturing mixed populations of T cytotoxic cells and MDSCs and reporting the effect of the latter on the former over time. Functionality of T reg cells should be also investigated in further studies.

Although it is impossible to extrapolate our results toward functionality, it is plausible that immune infiltrates characterized in this study may correspond to an immunosuppressive phenotype. Further work obviously needs to be done to conclude with any certainty the function of these populations. However, if they are immunosuppressive, there may be room for therapeutic approaches aiming to restore the immune function in sarcomas.

References

1. D'Acquisto F & Crompton T (2011). CD3+CD4-CD8- (double negative) T cells: Saviours or villains of the immune response? *Biochem Pharmacol*, 82(4):333-40.
2. Almand B, Clark JI, Nikitina E, van Beynen J, English NR, Knight SC et al. (2001). Increased production of immature myeloid cells in cancer patients: a mechanism of immunosuppression in cancer. *J Immunol*, 166(1):678-89.
3. Chanmee T, Ontong P, Konno K, Itano N (2014). Tumor-associated macrophages as major players in the tumor microenvironment. *Cancers (Basel)*, 6(3):1670-90.
4. Coussens LM & Werb Z (2002). Inflammation and cancer. *Nature*, 420(6917):860-7.
5. Danbara M, Yoshida M, Kanoh Y, Jiang SX, Masuda N, Akahoshi T, Higashihara M (2009). Flow cytometric detection of small cell lung cancer cells with aberrant CD45 expression in micrometastatic bone marrow. *Jpn J Clin Oncol*, 39(11):771-5.
6. Danese S & Rutella S (2007). The Janus face of CD4+CD25+ regulatory T cells in cancer and autoimmunity. *Curr Med Chem*, 14(6):649-66.
7. Davidoff AM (2012). Wilms tumor. *Adv Pediatr*, 59(1):247-67.
8. De Leeuw RJ, Kost SE, Kakal JA, Nelson BH (2012). The prognostic value of FoxP3+ tumor-infiltrating lymphocytes in cancer: a critical review of literature. *Clin Cancer Res*, 18(11):3022-9.
9. Gabrilovitch DI & Nagaraj S (2009). Myeloid-derived suppressor cells as regulators of the immune system. *Nat Rev Immunol*, 9(3):162-74.
10. Galon J, Costes A, Sanchez-Cabo F, Kirilovsky A, Mlecnik B, Lagorce-Pagès C et al. (2006). Type, Density, and Location of Immune Cells Within Human Colorectal Tumors Predict Clinical Outcome. *Science*, 313:1960-1964.
11. Galon J, Angell HK, Bedognetti D and Marincola FM (2013). The continuum of cancer immunosurveillance: prognostic, predictive, and mechanistic signature. *Immunity*, 39:11-26.
12. Gentles AJ, Newman AM, Liu CL, Bratman SV, Feng W, Kim D, Nair WS, Xu Y, Khuong A, Hoang CD, Diehn M, West RB, Plevritis SK & Alizadeh AA (2015). The prognostic landscape of genes and infiltrating immune cells across human cancers. *Nature Medicine*, 21(8):938-45.
13. Hanahan D & Weinberg RA (2000). The hallmarks of cancer. *Cell*, 100(1):57-70.
14. Hanahan D & Weinberg RA (2011). Hallmarks of cancer: the next generation. *Cell*, 144(5):646-74.

15. Hillhouse EE & Lesage S (2013). A comprehensive review of the phenotype and function of antigen-specific immunoregulatory double negative T cells. *J Autoimmun*, 40:58-65.
16. Johann PD, Vaegler M, Gieseke F, Mang P, Armeanu-Ebinger S, Kluba T et al. (2010). Tumour stromal cells derived from paediatric malignancies display MSC-like properties and impair NK cell cytotoxicity. *BMC Cancer*, 10:501.
17. Joyce JA & Pollard JW (2009). Microenvironmental regulation of metastasis. *Nat Rev Cancer*, 9(4):239-52.
18. Kerouanton A, Jimenez I, Cellier C, Laurence V, Helfre S, Pannier S et al. (2014). Synovial sarcoma in children and adolescents. *J Pediatr Hematol Oncol*, 36(4):257-62.
19. Kumar V, Abbas AK, Fausto N, Aster J. Robbins and Cotran Pathologic Basis of Disease, 8th Edition, Elsevier, 2010.
20. Kuonen F, Touvrey C, Laurent J, Ruegg C (2010). Fc block treatment, dead cells exclusion, and cell aggregates discrimination concur to prevent phenotypical artifacts in the analysis of subpopulations of tumor-infiltrating CD11b⁺ myelomonocytic cells. *Cytometry Part A*, 77A:1082-90.
21. Martinez FO & Gordon S (2014). The M1 and M2 paradigm of macrophage activation: time for reassessment. *F1000Prime Rep*, 6:13.
22. Mirza N, Fishman M, Fricke I, Dunn M, Neuger AM, Frost TJ et al. (2006). All-trans-retinoic acid improves differentiation of myeloid cells and immune response in cancer patients. *Cancer Res*, 66(18):9299-307.
23. Moretta L, Montaldo E, Vacca P, Del Zotto G, Moretta F, Merli P et al. (2014). Human Natural Killer Cells: Origin, Receptors, Function, and Clinical Applications. *Int Arch Allergy Immunol*, 164:253-264.
24. Prendergast GC & Jaffee EM. Cancer Immunotherapy: Immune Suppression and Tumor Growth. 2nd Edition, Academic Press, Elsevier, 2013.
25. Riggi N & Stamenkovic I (2007a). The biology of Ewing sarcoma. *Cancer Let*, 254(1):1-10.
26. Riggi N, Cironi L, Suva ML, Stamenkovic I (2007b). Sarcomas: genetics, signaling, and cellular origins. Part 1: The fellowship of TET. *J Pathol*, 213(1):4-20.
27. Ruffell B, Affara NI, Coussens LM (2012). Differential macrophage programming in the tumor microenvironment. *Trends Immunol*, 33(3):119-26.
28. Schmielau J & Finn OJ (2001). Activated granulocytes and granulocyte-derived hydrogen peroxide are the underlying mechanism of suppression of T-cell function in advanced cancer patients. *Cancer Res*, 61(12):4756-60.
29. Smith SC, Poznanski AA, Fullen DR, Ma L, McHugh JB, Lucas DR et al. (2013). CD34-positive superficial myxofibrosarcoma: a potential diagnostic pitfall. *J Cutan Pathol*, 40(7):639-45.

30. Solito S, Marigo I, Pinton L, Damuzzo V, Mandruzzato S, Bronte V (2014). Myeloid-derived suppressor cell heterogeneity in human cancers. *Ann N Y Acad Sci*, 1319:47-65.
31. Sorbye SW, Kilvaer T, Valkov A, Donnem T, Smeland E, Al-Shibli K, et al. (2011). Prognostic impact of lymphocytes in soft tissue sarcomas. *PLoS One*, 6(1):e14611.
32. Sorbye SW, Kilvaer TK, Valkov A, Donnem T, Smeland E, Al-Shibli K et al. (2012). Prognostic impact of peritumoral lymphocyte infiltration in soft tissue sarcomas. *BMC Clin Pathol*, 12:5.
33. Strachan DC, Ruffell B, Oei Y, Bissell MJ, Coussens LM, Pryer N and Daniel D. (2013). CSF1R inhibition delays cervical and mammary tumor growth in murine models by attenuating the turnover of tumor-associated macrophages and enhancing infiltration by CD8+ T cells. *Oncoimmunology*, 2:12, e26968.
34. Suva ML, Cironi L, Riggi N, Stamenkovic I (2007). Sarcomas, genetics, signaling, and cellular origins. Part 2: TET-independent fusion proteins and receptor tyrosine kinase mutations. *J Pathol*, 2013(2):117-30.
35. Thomson CW, Lee B, Zhang L (2006). Double-negative regulatory T cells: non-conventional regulators. *Immunol Res*, 34(1-2):163-78.
36. de Visser KE, Eichten A, Coussens LM (2006). Paradoxical roles of the immune system during cancer development. *Nat Rev Cancer*, 6(1):24-37.
37. Weinberg RA. *The Biology of Cancer*. 2nd Edition, Garland Science, 2013.
38. Wogan GN, Hecht SS, Feltron JS, Conney AH, Loeb LA (2004). Environmental and chemical carcinogenesis. *Semin Cancer Biol*, 14(6):473-86.
39. Young KJ, Kay LS, Philips MJ, Zhang Li (2003). Antitumor activity mediated by double-negative T cells. *Cancer Res*, 63(22):8014-21.
40. Young MR, Petruzzelli GJ, Kolesiak K, Achille N, Lathers DM, Gabrilovich DI (2001). Human squamous cell carcinomas of the head and neck chemoattract immune suppressive CD34(+) progenitor cells. *Hum Immunol*, 62(4):332-41.
41. Zea AH, Rodriguez PC, Atkins MB, Hernandez C, Signoretti S, Zabaleta J et al. (2005). Arginase-producing myeloid suppressor cells in renal cell carcinoma patients: a mechanism of tumor evasion. *Cancer Res*, 65(8):3044-8.